*Proc. Natl. Acad. Sci. USA*
Vol. 93, pp. 9858–9863, September 1996
Neurobiology

# Olfactory marker protein (OMP) gene deletion causes altered physiological activity of olfactory sensory neurons

**(olfactory bulb/tyrosine hydroxylase/cholecystokinin/electroolfactogram)**

O. I. BUIAKOVA*†, H. BAKER‡, J. W. SCOTT§, A. FARBMAN¶, R. KREAM‖, M. GRILLO*, L. FRANZEN‡, M. RICHMAN¶, L. M. DAVIS§, S. ABBONDANZO*, C. L. STEWART*, AND F. L. MARGOLIS*,**

*Roche Institute of Molecular Biology, Roche Research Center, Nutley, NJ 07110; ‡Burke Rehabilitation Center, Cornell University Medical College, White Plains, NY 10605; §Department of Anatomy and Cell Biology, Emory University, Atlanta, GA 30322; ¶Department of Neurobiology and Physiology, Northwestern University, Evanston, IL 60208; and ‖Tufts New England Medical Center, Boston, MA 02111

*Communicated by Sidney Udenfriend, Roche Institute of Molecular Biology, Nutley, NJ, June 11, 1996 (received for review January 10, 1996)*

ABSTRACT **Olfactory marker protein (OMP) is an abundant, phylogenetically conserved, cytoplasmic protein of unknown function expressed almost exclusively in mature olfactory sensory neurons. To address its function, we generated OMP-deficient mice by gene targeting in embryonic stem cells. We report that these OMP-null mice are compromised in their ability to respond to odor stimuli, providing insight to OMP function. The maximal electroolfactogram response of the olfactory neuroepithelium to several odorants was 20–40% smaller in the mutants compared with controls. In addition, the onset and recovery kinetics following isoamyl acetate stimulation are prolonged in the null mice. Furthermore, the ability of the mutants to respond to the second odor pulse of a pair is impaired, over a range of concentrations, compared with controls. These results imply that neural activity directed toward the olfactory bulb is also reduced. The bulbar phenotype observed in the OMP-null mouse is consistent with this hypothesis. Bulbar activity of tyrosine hydroxylase, the rate limiting enzyme of catecholamine biosynthesis, and content of the neuropeptide cholecystokinin are reduced by 65% and 50%, respectively. This similarity to postsynaptic changes in gene expression induced by peripheral olfactory deafferentation or naris blockade confirms that functional neural activity is reduced in both the olfactory neuroepithelium and the olfactory nerve projection to the bulb in the OMP-null mouse. These observations provide strong support for the conclusion that OMP is a novel modulatory component of the odor detection/signal transduction cascade.**

Odor detection occurs in olfactory cilia where signal transduction is believed to be initiated by a stimulus molecule interacting with a seven-transmembrane domain G protein-coupled receptor. Subsequent activation of G protein-mediated second messenger systems leads to cation channel opening and action potential generation (1). Many proteins of the odor detection/signal tranduction cascade are either abundantly or selectively expressed in olfactory sensory neurons (1–4). Although these proteins are structurally homologous to proteins involved in signal transduction in other cell types, attempts to demonstrate functional activity of olfactory receptor molecules in heterologous systems have been largely unsuccessful (see, however, ref. 5). The basis for this lack of success is unknown but may relate to the difficulty in choosing an optimal stimulus/receptor pair. This is unlikely, as individual olfactory sensory cells, expressing one or few receptor types (1, 6, 7), respond to a wide range of stimuli (1, 8, 9). Other possibilities include the absence in heterologous systems of essential olfactory neuron-specific components directly or indirectly involved in odor detection/signal transduction processes. These latter components might include proteins selectively expressed in mature olfactory sensory neurons and their cilia. The olfactory marker protein (OMP) is a possible candidate because this 19-kDa phylogenetically conserved, cytoplasmic protein is expressed almost exclusively by mature olfactory neurons in essentially all vertebrate species (10, 11). OMP is present throughout the cytoplasm of olfactory sensory neurons and is abundant in the olfactory ciliary lumen (10, 12). Here we report that olfactory sensory neurons of OMP-null mice, from which the OMP gene has been deleted by homologous recombination in embryonic stem (ES) cells, have reduced electrophysiological activity. Furthermore, this reduction in neural activity of olfactory neurons influences downstream gene expression in the olfactory bulbs.

## MATERIALS AND METHODS

**Targeting Vector.** The mouse OMP targeting construct contained 9 kb of 5′ and 1.5 kb of 3′ homology, along with PGK-neomycin resistance (PGK-neo) and herpes simplex virus-thymidine kinase (HSV-TK) cassettes in pBluescript KS(+) (Stratagene) as illustrated (see Fig. 1).

**Generation of Chimeric Mice.** ES cell line W9.5 was grown on a feeder layer of mitomycin C-inactivated primary mouse embryonic fibroblasts in Dulbecco's modified Eagle's medium supplemented with 20% (vol/vol) fetal bovine serum and 0.1 mM 2-mercaptoethanol. The cells were electroporated with 25 μg of linearized vector and clones selected using positive (PGK-neo) and negative (HSV-TK) selection with G418 and 1-(2′-deoxy-2′-fluoro-1-beta-D-arabinofuranosyl)-5-iodouracil (FIAU), respectively, as described (13). *Eco*RI diagnostic restriction enzyme digests of DNA from surviving clones were screened for homologous recombination by Southern analysis using the 3′ single copy probe (see Fig. 1*a*). The overall targeting frequency was 10% of clones surviving double selection. Following verification of homologous recombination, cells from two clones (see Fig. 1*b*) were used to generate chimeric mice (13). Germ-line transmission of the targeted allele was monitored by Southern analysis as above and by PCR. Tail tip DNA preparations and PCR were performed as described (14). The wild-type OMP allele was detected using a 5′ primer homologous to DNA sequence in the coding region of the OMP gene (5′-AAGCTGCAGTTCGATCACTGGA-3′) and a 3′ primer (5′-TGTTCCTGTCCAGTCTCAGTCT-

The publication costs of this article were defrayed in part by page charge payment. This article must therefore be hereby marked "*advertisement*" in accordance with 18 U.S.C. §1734 solely to indicate this fact.

Abbreviations: OMP, olfactory marker protein; CCK, cholecystokinin; ES, embryonic stem cell; EOG, electroolfactogram.

†Present address: Departments of Psychiatry and Genetics, Columbia University, New York Psychiatric Institute Unit 58, 722 West 168 Street, New York, NY 10032.

**To whom reprint requests should be sent at the present address: Department of Anatomy, University of Maryland School of Medicine, 685 West Baltimore Street, Baltimore, MD 21201. e-mail: fmargoli@umabnet.ab.umd.edu.

3′) homologous to the 3′ untranslated portion of the OMP gene transcript that lies within the 3′ homology region of the targeting construct. The targeted OMP allele was identified by using a 5′ primer homologous to the promoter region of the neo gene (5′-TACCGGTGGATGTGGAATGTGT-3′) and the same 3′ primer as for the wild-type OMP allele above. A 700-bp amplicon was generated in the presence of the wild-type allele and a 390-bp amplicon in the presence of the targeted allele.

**Western Blot Analysis.** Mice were sacrificed by $CO_2$ and exsanguination, and olfactory mucosa and bulbs were dissected, frozen, weighed, and homogenized in SDS buffer (1% SDS/10 mM Tris·HCl, pH 7.4/100 μM NaF/10 mM sodium pyrophosphate/10 μg of aprotinin per ml/5 mg of leupeptin per ml/0.2 mM phenylmethylsulfonyl fluoride). Aliquots were electrophoresed in 15% polyacrylamide gels, transferred to 0.45 μm nitrocellulose, blocked with 5% nonfat milk and 0.5% BSA in PBST (137 mM NaCl/2.5 mM KCl/10 mM $Na_2HPO_4$/1.75 mM $KH_2PO_4$, pH 7.2/0.25% Tween 20), and sequentially incubated with 1/250 rabbit-anti-OMP, 1/1000 goat anti-rabbit-IgG phosphatase conjugated; the color was developed with 100 mg of nitroblue tetrazolium per ml and 50 mg/ml of X-phosphate (Boehringer Mannheim).

**Immunocytochemistry.** Olfactory epithelia from mice at 2 days and 2 months postnatal were fixed in Zamboni's fixative, cryoprotected in 30% sucrose and frozen in OCT (Tissue Tech, Miles). The tissue blocks were sectioned at 8 to 10 μm at −20°C. The sections were washed in PBS containing 0.2% glycine, incubated with goat polyclonal anti-OMP antibodies (1:1000) or rabbit polyclonal anti-carnosine antibodies (1:500) overnight at room temperature, and washed in PBS. Anti-OMP-treated sections were incubated with rhodamine-conjugated donkey anti-goat IgG antibodies (1:80) (Chemicon); anti-carnosine treated sections were incubated with fluorescein isothiocyanate-conjugated swine anti-rabbit IgG antibodies (1:40) (Dako). In both cases incubations were performed for 1 hr at room temperature in the dark with subsequent washes in PBS.

**Histology.** Olfactory epithelia from 3-month-old mice were fixed in Bouin's fixative and decalcified with RDO (Apex Engineering, Plainfield, IL). The samples were dehydrated, embedded in paraffin, and sectioned at 6–8 μm. Sections were deparaffined, rehydrated, and stained with hematoxylin/eosin. To count dendritic knobs, olfactory tissue from 5-week-old mice (two wild type, three heterozygotes, and three OMP-null mice) was fixed in 0.1 M sodium phosphate (pH 7.2) containing 1.6% formaldehyde and 2% glutaraldehyde at 4°C. The tissue was subsequently processed and embedded in an epon-araldite plastic mixture. Olfactory knobs were counted either from six nonadjacent sections in each of two areas per mouse for a total olfactory epithelial length of ≈20 microns (electron microscope) or in three to four nonadjacent sections from each of four areas per mouse along 200–600 μm of olfactory epithelial length (light microscope). In total, ≈400–500 knobs were counted per mouse in light and electron microscopy, representing 1.5–2.0 mm of epithelial length.

**Biochemistry.** Mice, at 1 and 2 months postnatal, were sacrificed by $CO_2$ inhalation followed by exsanguination; the olfactory bulbs were dissected individually, frozen on dry ice, coded, and weighed. Single olfactory bulbs from each pair were homogenized in 5 mM potassium phosphate buffer (pH 7.0) containing 0.2% Triton X-100; tyrosine hydroxylase activity and protein content were determined as described (15). In the assay $^{14}$C-dopa generated from $^{14}$C-tyrosine substrate is separated on alumina, quantified by scintillation spectrometry, and reported as nmol dopa/bulb/15 min. For quantification of levels of cholecystokinin (CCK)-like immunoreactivity (CCK-LI) by RIA, the second member of each pair of frozen olfactory bulbs, stored at −80°C, was extracted using procedures previously described in detail (16). Briefly, bulbs were each homogenized in 2 M acetic acid followed by the addition of 20 volumes of cold 50% acetonitrile/0.1% trifluoroacetic acid. Following centrifugation (10,000 × *g* for 30 minutes), the peptide-containing supernatants were subsequently delipidated and concentrated. The acidified upper aqueous phase was dried and reconstituted in RIA buffer. Overall, this simple extraction procedure yields recoveries of exogenously added CCK >90%.

The RIA procedure for quantification of CCK-LI uses a highly selective antiserum generated against synthetic sulfated CCK-8 coupled to keyhole limpet hemocyanin using previously described conjugation procedures (16). The antibody recognizes sulfated CCK-8 and sulfated gastrin 17 on an equimolar basis, with nonsulfated CCK-8 and gastrin 17 displaying <10% cross-reactivity. Other methionine-containing neuropeptides such as substance P, methionine enkephalin, and β-endorphin display <0.1% cross-reactivity in the RIA. The RIA tracer is a radioiodinated CCK-Bolton Hunter reagent conjugate, prepared by previously described procedures and purified by HPLC. In the RIA, partially purified CCK antiserum is used at a final dilution of 1:20,000 at which 35% of the added radiolabeled peptide is specifically bound. Initial incubation with the antibody is for 24 hr, followed by addition of 20,000 cpm of $^{125}$I-labeled CCK tracer and an additional 24-hr incubation. Finally, precipitation of antibody-bound radioactive tracer is achieved by addition of 1 ml of cold absolute ethanol. After centrifugation, supernatants are aspirated and the pellets counted in a γ counter at >70% efficiency. Nonspecific binding of radiolabel is typically 2% and is subtracted from each tube. For unknown samples, peptide concentrations are quantified by interpolation from a logit-log plot of the standard dose-response displacement curve which utilizes synthetic sulfated CCK-8 as the RIA standard. In these analyses, the lowest detectable dose is ≈1 fmol peptide/tube and 50% displacement is achieved at ≈12 fmol peptide/tube.

**Electrophysiology.** Male and female mice (20–35 g, 10–14 weeks old) were anesthetized with nembutal (70 mg/kg) or sacrificed by $CO_2$ inhalation. A cannula was placed in the trachea to allow stimuli to be aspirated through the nose at 50 ml/min. The nonluminal side (lamina propria) of the olfactory epithelium was exposed by drilling through the bone with a dental burr. Two exposures were made in each animal, one in the dorsal recess of the epithelium and one in the lateral recess between the base of the turbinate bones. Recordings were made with micropipettes (resistance 5–10 mΩ) filled with Ringer's solution and driven through the epithelium until a large negative response was evoked by odor stimulation. Clean air flowed into a chamber in front of the nose at 500 ml/min. Air saturated with odors was injected into the chamber by a computer controlled syringe pump. The rate of flow produced by the syringe pump determines the odor concentration (expressed as percent of vapor saturation). All odors were routinely tested at 2, 7, and 18% of saturation. Each odor presentation was accomplished by infusion of compound into the stimulus chamber 10 sec before the beginning of an artificial sniff produced by opening a valve in the vacuum line connected to the tracheal cannula. This preparation is similar to that previously described (17). One-minute intervals elapsed between odor presentations. Isoamyl acetate was always the first odor tested, and these data were used for comparisons of kinetics. The same results were observed with either anesthetized or $CO_2$-killed mice, but only data from the latter were used for the analysis of responses to single pulses (see Fig. 3 *a* and *c*). These data were evaluated by analysis of variance across OMP status, electrode position, and stimulus concentration. Recordings of responses to dual odor pulses were made primarily from the dorsal recess. Results from some anesthetized mice were included in this analysis. Analysis of

variance showed that the difference between anesthetized and killed mice was not a significant contribution to the variance.

## RESULTS AND DISCUSSION

To address the function of OMP, we used gene targeting in mouse ES cells to generate a null allele by replacing the intronless coding region of the OMP gene (11) with a selection cassette containing the neomycin phosphotransferase (*neo*) gene (Fig. 1 *a* and *b*). The absence of OMP expression in mice homozygous for the targeted allele was confirmed immunochemically (Figs. 1*c* and 2 *c* and *e*). Central nervous system areas of ectopic OMP expression (18) were also devoid of OMP (not shown). Quantification of OMP levels by ELISA revealed that heterozygous mutant mice had 40–50% of the

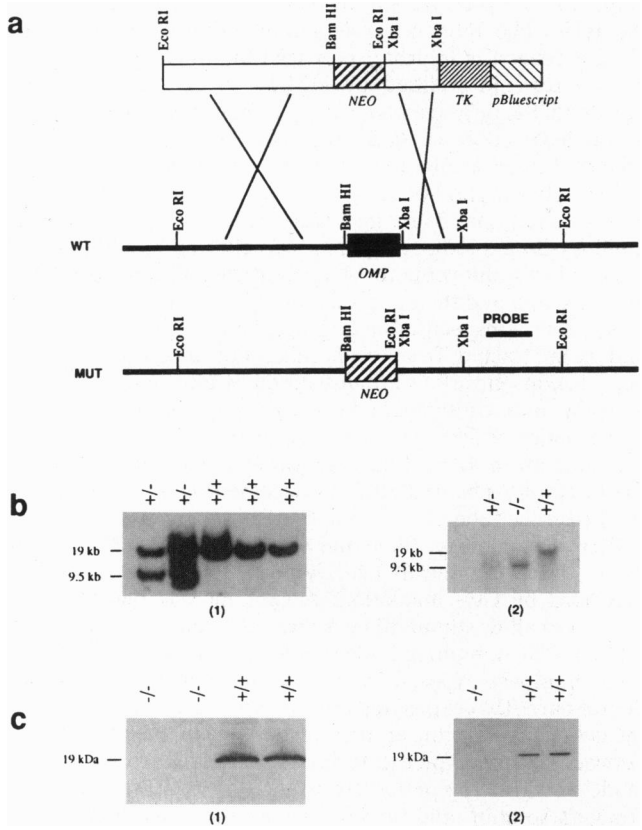


FIG. 1. Gene targeting at the mouse OMP locus. (*a*) Schematic representation of the OMP targeting vector (*Top*), the OMP locus (*Middle*), and the expected recombination events (*Bottom*). Successful gene replacement by the targeting vector results in the deletion of the entire coding region of the OMP gene and insertion of a PGK-neo selection cassette in the opposite orientation. The location of the DNA probe used to identify putative targeted ES cell clones and their progeny is indicated. (*b*) Southern blot analysis of gene targeting at the OMP locus and transmission of the targeted allele. (*1*) A 19-kb *Eco*RI fragment, indicative of a wild-type allele, is detected in the parental ES cell line (+/+). An additional fragment of 9.5 kb corresponding to the targeted allele, is detected in DNA from two clones (−/+). Each of these clones was used to generate an independent OMP-null line. Most of the data presented here derive from analysis of one of these two lines. (*2*) The three lanes represent DNA samples from tail tips of 3-week-old heterozygous (−/+), homozygous mutant (−/−), and wild-type (+/+) progeny derived from intercrosses between mice heterozygous for the targeted allele. (*c*) Western immunoblot analysis of extracts from olfactory epithelium (*1*) and olfactory bulbs (*2*) of mice that are genotypically wild-type (+/+), or homozygous (−/−) for the targeted OMP locus. Goat anti-OMP antiserum identifies the 19-kDa OMP in wild type but not in homozygous OMP-null mice. In wild-type olfactory bulbs OMP is present only in axon terminals of olfactory sensory neurons but not in any bulbar cells.

OMP level of wild-type littermates indicating that each allele is autonomous. Immunoblots probed with antiserum directed against $G_{olf}$, a component of the olfactory transduction cascade, indicated that there was no difference in $G_{olf}$ expression between the wild-type and OMP-null mice. This observation suggests that OMP gene deletion was not accompanied by global alterations in gene expression.

Before analysis of the OMP-null mice for potential functional deficits, it was essential to evaluate the morphological organization of the olfactory neuroepithelium in the OMP-null mice to determine if there were any gross anatomical abnormalities that could compromise interpretation of the functional studies. To characterize the morphological organization of the olfactory epithelium in the OMP-null mice, histological, immunocytochemical, and electron microscopy analyses were performed. Hematoxylin/eosin-stained histological sections of olfactory mucosa from mutant and wild-type siblings were indistinguishable (Fig. 2 *a* and *b*). The ratio of immature to mature sensory neurons seemed to be unaffected. Immunostaining with anticarnosine antibodies (Fig. 2 *d* and *f*), that stain mature olfactory sensory neurons (19), or with anti-GAP43 antibodies (not shown), that identify immature neurons (20), was similar in OMP-null and wild-type mice despite the absence of any OMP in the OMP-null mice (Fig. 2). Quantification of the olfactory epithelial dendritic knob density (by electron microscopy and light microscopy of plastic sections) was the same for OMP-null and wild-type controls ($31 \pm 5.5/200$ microns and $33 \pm 3.6/200$ microns, respectively). A dendritic knob decorated by long cilia at the surface of the epithelium and the formation of synaptic contact with target neurons in the bulb are key morphological characteristics of a mature olfactory sensory neuron (1). Our electron microscopy, histological, and immunocytochemical observations demonstrate that the olfactory neuroepithelium of the OMP-null mice appears morphologically normal.

We recorded electroolfactograms (EOGs) from the olfactory epithelium of wild-type and OMP-null mice to evaluate their responses to odors (Fig. 3*a*). For the initial tests with isoamyl acetate, the response magnitudes (Fig. 3*b*) were 25% lower in the OMP-null mice. Responses to all other odor chemicals tested (benzaldehyde, menthone, benzene, limonene, and cyclooctane) were also 20–40% smaller in the OMP-null mice (data not shown). These decreases were statistically significant ($P < 0.02$) for all except limonene and cyclooctane. We observed large effects of the mutation on response kinetics. The slopes of the initial and decay phases of the response to isoamyl acetate (Fig. 3*b*) were 53% and 43% smaller in the mutant mice, indicating that both response generation and recovery processes are compromised in the olfactory epithelium of OMP-nulls (Fig. 3 *a* and *b*). The initial response slopes were significantly slower ($P < 0.05$) for all odors tested. To further test the impairment in response recovery, we analyzed the responses to two successive pulses of isoamyl acetate separated by a 6-sec interval. Recovery of the response was substantially slower for the OMP-null mice at five different concentrations (Fig. 3 *c* and *d*). This diminished recovery probably leads to a sustained reduction in response to repeated sniffs that is far greater than the 25% smaller response that we observed with single pulse stimulation. In the OMP-null mice, the reductions in magnitude of the initial EOG response, the alterations in the kinetics, and the relative magnitude decrement in response to successive stimulus pulses all indicate that the olfactory neuroepithelium is severely compromised in its ability to respond to, and recover from, odor stimulation.

Is this deficit in the ability of olfactory sensory neurons to respond to odor stimulation also reflected in a decreased ability to communicate with their neuronal targets in the olfactory bulb? Mature olfactory sensory neurons synapse on intrinsic bulbar neurons whose morphological and biochemical

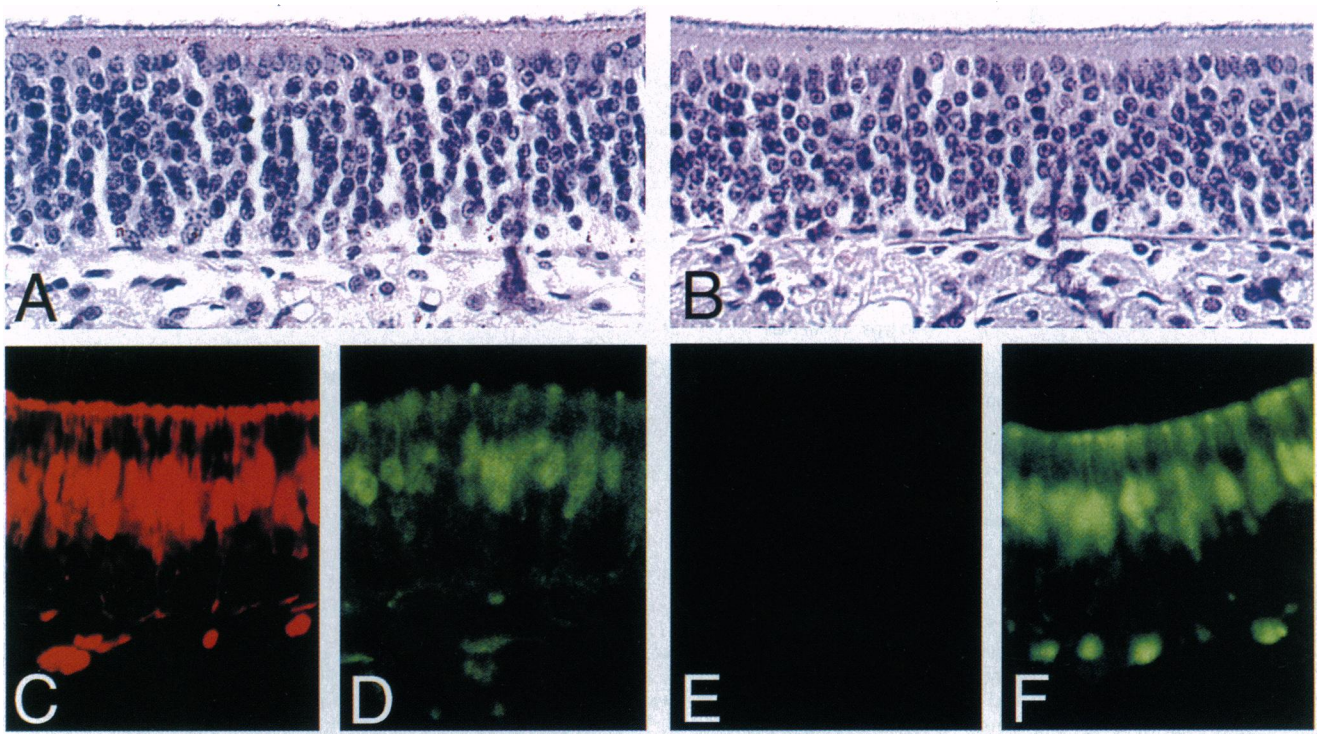


FIG. 2. OMP deletion does not cause morphological alteration in the mutant olfactory neuroepithelium. (*a* and *b*) Histological sections of the olfactory mucosa from wild-type (*a*) and homozygous mutant (*b*) mice. (*c–f*) Only mature olfactory sensory neurons are revealed by anti-OMP antibodies in wild-type (*c*) and by anticarnosine antibodies in wild-type (*d*), and mutant (*f*) mice. No anti-OMP immunostaining was observed in the mutant neuroepithelium (*e*). The occurrence of mature olfactory sensory neurons seems to be unaffected in the mutant olfactory neuroepithelium.

status is indicative of the functional state of this connection. Therefore, it was of interest to evaluate the influence of the OMP-deficient synapses on gene expression by intrinsic bulbar neurons. We determined olfactory bulbar tyrosine hydroxylase activity and CCK content to monitor intrinsic bulbar neuron responses. The olfactory bulbs of the OMP-null mice manifested changes similar to those in the bulbs of deafferented or odor-deprived animals (Table 1). Olfactory bulb weight was about 15% less in OMP-null mice compared with age-matched wild-type siblings. This small but significant difference was observed in mice at 1 and 2 months postnatal. More striking was the effect of the absence of OMP on the levels of tyrosine hydroxylase activity and CCK in the olfactory bulbs. Both tyrosine hydroxylase activity per bulb and CCK content per bulb were reduced by 65% and 40–50%, respectively, compared with wild-type mice (Table 1). The qualitative similarity between the olfactory bulb phenotype in the OMP-null mice and that seen in bulbs of wild-type mice following deafferentation or odor deprivation (21–24) suggests that in all these situations the same mechanism is involved—i.e., a reduction of the afferent input from the olfactory neuroepithelium to the olfactory bulb.

These electrophysiological and biochemical analyses of the OMP-null mouse provide a functional demonstration of the role of OMP in olfactory neurons and imply that OMP is a novel modulator of the signal detection/transduction cascade in the olfactory sensory neuron.

In view of the decrement in olfactory neuron function in the OMP-null mice, is the behavior of the OMP-null mice compromised? Curiously, mice homozygous for the disrupted allele showed no behavioral evidence of anosmia. Despite the dependence of neonatal mice on olfactory function for nipple location, attachment and suckling (28), OMP-null mice appear behaviorally and anatomically normal at birth. Although olfactory cues modulate the development and expression of sexual and social behavior in mice (26, 28), adult OMP-null mice breed, deliver, and raise pups that are themselves fertile. Further, their open field exploratory activity is the same as that of wild-type controls (data not shown). Two simple behavioral tests confirm the ability of the null-mutants to detect and discriminate odors. First, the time required to find a hidden food pellet after overnight food deprivation (27) is the same for homozygous OMP-null and wild type mice [60 ± 40 sec ($n$ = 40) versus 80 ± 40 sec ($n$ = 22), respectively; mean ± SD]. Second, in contrast to anosmic males (25), mature OMP-null males from different litters fight when caged together, indicating their ability to identify each other as strangers. However, under laboratory conditions the olfactory system is barely

Table 1. Characterization of the olfactory bulbs from OMP-null and wild-type mice

| Age, month | Bulb weight, mg ± SD | | | TH activity, nmol/bulb/15 min ± SD | | | CCK content, fmol/bulb ± SD | | |
|---|---|---|---|---|---|---|---|---|---|
| | OMP-null | Wild type | *P* | OMP-null | Wild type | *P* | OMP-null | Wild type | *P* |
| 1 | 8.6 ± 1.1 | 10.7 ± 0.6 | <0.01 | 0.16 ± 0.06 | 0.30 ± 0.08 | <0.05 | ND | ND | |
| 2 | 12.4 ± 0.9 | 14.8 ± 0.5 | <0.004 | 0.12 ± 0.04 | 0.34 ± 0.09 | <0.002 | 675 ± 176 | 1540 ± 173 | <0.002 |

One- and 2-month-old postnatal mice were tested. Each group consisted of four or five OMP-null and four or five wild-type mice of the same age. The mice in each group derived from intercrosses between mice heterozygous for the targeted OMP allele and were littermates or were born from sibling parents. In each group the mice were born within 4 days of each other. Since murine olfactory bulbs continue to increase in size during the first 3–4 postnatal months the absolute mean values for bulb weight and tyrosine hydroxylase (TH) activity per bulb differ in both wild-type and the mutant animals from group to group. ND, not determined.

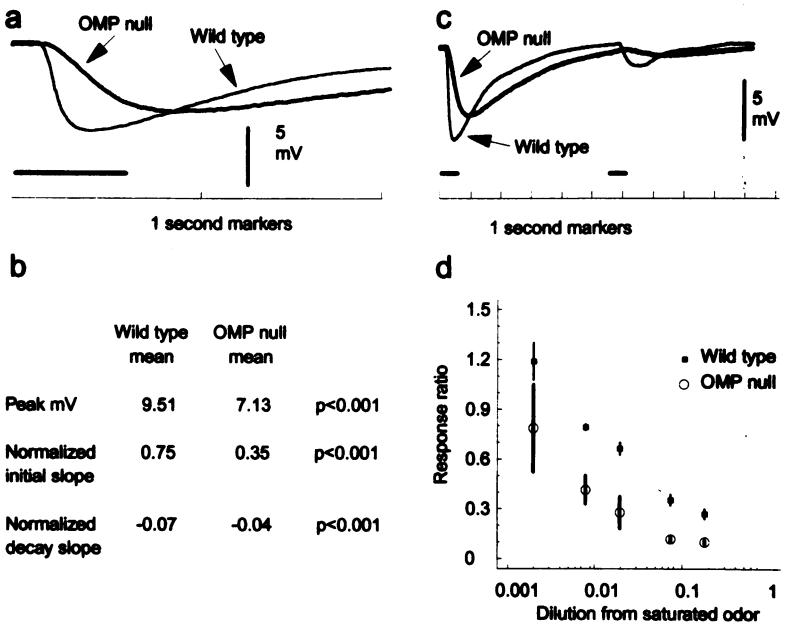


| | Wild type mean | OMP null mean | |
|---|---|---|---|
| Peak mV | 9.51 | 7.13 | p<0.001 |
| Normalized initial slope | 0.75 | 0.35 | p<0.001 |
| Normalized decay slope | -0.07 | -0.04 | p<0.001 |

FIG. 3. EOG responses evoked in OMP-null and wild-type mice by isoamyl acetate. (*a*) Responses at the dorsomedial recording site to a single pulse of isoamyl-acetate at 7% of saturation at room temperature (onset and duration indicated by the solid bar). The thicker trace is from an OMP-null and the thin trace is from a wild-type mouse. Positive is upward. Note that both the initial response and return to baseline are more rapid for the wild-type mice. (*b*) Summary of peak voltages and time courses of responses for all recording sites to single pulses of isoamyl acetate. The normalized slope was calculated by dividing the slope of the steepest portion of the response by the peak voltage. This normalization corrected the initial and decay slopes for response size. This method of comparison of response kinetics was more accurate than measurement of time to peak because of difficulty in measuring the slow response peaks (see *a*). (*c*) Responses of an OMP-null mouse (thicker trace) and a wild-type mouse (thin trace) to two successive pulses of isoamyl acetate separated by a 6-sec interval. Stimulus parameters were as in *a*. (*d*) Means and standard errors for the second response (as in *c*) as a fraction of the first response. Closed circles, wild-type mice ($n = 10$), and open circles, OMP-null mice ($n = 4$), recorded at the dorsomedial position. There was no significant difference in these curves for the lateral recording position ($n = 3$). The overall difference attributable to OMP status was significant at $P < 0.01$ by analysis of variance.

challenged. For example, rodents with >90% of their olfactory epithelium or olfactory bulbs destroyed can still detect and discriminate odors (25–27). The EOG data suggest an explanation for these observations. First, they demonstrate that, although the olfactory sensory neurons of OMP-null mice are functionally compromised, they are still responsive. Second, the EOG response decrements that we have observed are to repetitive stimulation with a single pure odor. In contrast, the behaviors we monitored are in response to complex odor mixtures. Alternatively, the OMP-null mice may have adopted subtle, novel behavioral strategies (e.g., altered sniff frequency) to compensate for their profound deficit to repetitive stimulation. Detailed behavioral evaluation of these mice will be critical to our understanding in the future.

In conclusion, our biochemical and physiological analyses of the OMP-null mouse provide insight into the enigmatic role of this protein in the function of the olfactory neuron. The OMP-null mice exhibit a defect in the EOG characterized by a reduction in the initial stimulus responsivity of the olfactory epithelium to odors, altered kinetics of response generation and recovery, and a reduced ability to respond to the second stimulus of a pair. These observations imply that overall there is a reduction of neural activity in the olfactory projection to the bulb. Consistent with this prediction, the profile of reduced gene expression in intrinsic olfactory bulb neurons is similar to that seen in animals after either deafferentation or naris closure, and reflects the reduced neural activity of the olfactory sensory neurons. This bulbar phenotype independently supports the conclusion that the OMP-null phenotype is characterized by a dramatic reduction in neural activity in the olfactory nerve to bulb projection. Together these independent observations are consistent with the compelling conclusion that OMP is a novel modulator of the signal detection/transduction cascade in the olfactory sensory neuron.

This work was supported in part by grants from the National Institutes on Aging (H.B.), the National Institute on Deafness and Other Communication Disorders (A.F. and J.W.S.), and the National Institiute on Drug Abuse (R.K.).

1. Shepherd, G. M. (1994) *Neuron* **13,** 771–790.
2. Buck, L. & Axel, R. (1991) *Cell* **65,** 175–187.
3. Reed, R. R. (1992) *Neuron* **8,** 205–209.
4. Liman, E. R. & Buck, L. B. (1994) *Neuron* **13,** 611–621.
5. Raming, K., Krieger, J., Strotmann, J., Boekhoff, I., Kubick, S., Baumstrack, C. & Breer, H. (1993) *Nature (London)* **361,** 353–356.
6. Chess, A., Simon, I., Cedar, H. & Axel, R. (1994) *Cell* **78,** 823–834.
7. Ressler, K. J., Sullivan, S. L. & Buck, L. B. (1994) *Curr. Opin. Neurobiol.* **4,** 588–596.
8. Ivanova, T. T. & Caprio, J. (1993) *J. Gen. Physiol.* **102,** 1085–1105.
9. Sicard, G. & Holley, A. (1984) *Brain Res.* **292,** 283–296.
10. Margolis, F. L. (1980) in *Proteins of the Nervous System*, eds. Bradshaw, R. A. & Schneider, D. M. (Raven, New York), pp. 59–84.
11. Buiakova, O. I., Rama Krishna, N. S., Getchell, T. V. & Margolis, F. L. (1994) *Genomics* **20,** 452–462.
12. Menco, B. P. (1989) *Cell Tissue Res.* **256,** 275–281.
13. Lau, M. M., Stewart, C. E., Liu, Z., Bhatt, H., Rotwein, P. & Stewart, C. L. (1994) *Genes Dev.* **8,** 2953–2963.
14. Kudrycki, K., Stein-Izsak, C., Behn, C., Grillo, M., Akeson, R. & Margolis, F. L. (1993) *Mol. Cell. Biol.* **13,** 3002–3014.
15. Joh, T. H., Geghman, C. & Reis, D. J. (1973) *Proc. Natl. Acad. Sci. USA* **70,** 2667–2771.
16. Shimonaka, H., Marchand, J. E., Connelly, C. S. & Kream, R. (1992) *J. Neurochem.* **59,** 81–92.
17. Ezeh, P. I., Davis, L. M. & Scott, J. W. (1995) *J. Neurophysiol.* **73,** 2207–2220.
18. Baker, H., Grillo, M. & Margolis, F. L. (1989) *J. Comp. Neurol.* **285,** 246–261.
19. Biffo, S., Grillo, M. & Margolis, F. L. (1990) *Neuroscience* **35,** 637–651.

20. Verhaagen, J., Oestreicher, A. B., Gispen, W. H. & Margolis, F. L. (1989) *J. Neurosci.* **9,** 683–691.
21. Baker, H., Morel, K., Stone, D. M. & Maruniak, J. A. (1993) *Brain Res.* **614,** 109–116.
22. Baker, H., Towle, A. C. & Margolis, F. L. (1988) *Brain Res.* **450,** 69–80.
23. Ehrlich, M. E., Grillo, M., Joh, T. H., Margolis, F. L. & Baker, H. (1990) *Mol. Brain Res.* **7,** 115–122.
24. Henegar, J. R. & Maruniak, J. A. (1991) *Brain Res.* **568,** 230–234.
25. Liebenauer, L. L. & Slotnick, B. M. (1996) *Physiol. Behav.*, in press.
26. Doty, R. L. (1986) *Experientia* **42,** 257–271.
27. Harding, J. W., Getchell, T. V. & Margolis, F. L. (1978) *Brain Res.* **140,** 271–285.
28. Blass, E. M. & Teicher, M. H. (1980) *Science* **210,** 15–22.